New Journal of Physics
The open-access journal for physics

Space and time resolved measurements of the heating of solids to ten million kelvin by a petawatt laser

M Nakatsutsumi[1], J R Davies[2,15], R Kodama[1,3], J S Green[4,5], K L Lancaster[4], K U Akli[6], F N Beg[7], S N Chen[7], D Clark[8], R R Freeman[8], C D Gregory[9], H Habara[1,3], R Heathcote[4], D S Hey[10,11], K Highbarger[8], P Jaanimagi[12], M H Key[10], K Krushelnick[5,13], T Ma[7], A MacPhee[10], A J MacKinnon[10], H Nakamura[1], R B Stephens[6], M Storm[12], M Tampo[3,14], W Theobald[12], L Van Woerkom[8], R L Weber[8], M S Wei[7], N C Woolsey[9] and P A Norreys[4,5]

[1] Graduate School of Engineering, Osaka University, 2-1 Yamada-oka, Suita, Osaka 565-0871, Japan
[2] GoLP, IPFN, Instituto Superior Técnico, 1049-001 Lisboa, Portugal
[3] Institute of Laser Engineering, Osaka University, 2-6 Yamada-oka, Suita, Osaka 565-0871, Japan
[4] STFC Rutherford Appleton Laboratory, Chilton, Oxon, OX11 0QX, UK
[5] Blackett Laboratory, Imperial College London, Prince Consort Road, London SW7 2BZ, UK
[6] General Atomics, PO Box 86508, San Diego, CA 92186-5608, USA
[7] Department of Mechanical and Aerospace Engineering, University of California San Diego, 9500 Gilman Drive 0411, La Jolla, CA 92093-0411, USA
[8] Department of Physics, Ohio State University, Columbus, OH 43200-1117, USA
[9] Department of Physics, University of York, Heslington, York YO10 5DD, UK
[10] Lawrence Livermore National Laboratory, PO Box 808, Livermore, CA 94550, USA
[11] Department of Applied Sciences, University of California, 1 Shields Avenue, Davis, CA 95616-8254, USA
[12] Laboratory of Laser Energetics, University of Rochester, 250 East River Road, Rochester, NY 14623, USA
[13] Center for Ultrafast Optical Science, University of Michigan, Ann Arbor, MI 48109, USA
[14] Kansai Photon Science Institute, Japan Atomic Energy Agency, Kyoto 619-0215, Japan
E-mail: jrd@ist.utl.pt

[15] Author to whom any correspondence should be addressed.

1367-2630/08/043046+13$30.00

New Journal of Physics **10** (2008) 043046 (13pp)
Received 21 February 2008
Published 24 April 2008
Online at http://www.njp.org/
doi:10.1088/1367-2630/10/4/043046

Abstract. The heating of plane solid targets by the Vulcan petawatt laser at powers of 0.32–0.73 PW and intensities of up to 4×10^{20} W cm^{-2} has been diagnosed with a temporal resolution of 17 ps and a spatial resolution of 30 μm, by measuring optical emission from the opposite side of the target to the laser with a streak camera. Second harmonic emission was filtered out and the target viewed at an angle to eliminate optical transition radiation. Spatial resolution was obtained by imaging the emission onto a bundle of fibre optics, arranged into a one-dimensional array at the camera entrance. The results show that a region 160 μm in diameter can be heated to a temperature of $\sim 10^7$ K ($kT/e \sim$ keV) in solid targets from 10 to 20 μm thick and that this temperature is maintained for at least 20 ps, confirming the utility of PW lasers in the study of high energy density physics. Hybrid code modelling shows that magnetic field generation prevents increased target heating by electron refluxing above a certain target thickness and that the absorption of laser energy into electrons entering the solid target was between 15–30%, and tends to increase with laser energy.

Contents

1. Introduction 2
2. Experimental methods 3
3. Results and discussion 5
4. Numerical modelling 8
5. Conclusions 11
Acknowledgments 12
References 12

1. Introduction

Lasers can now achieve petawatt powers (10^{15} W) and can be focused to spots a few microns (10^{-6} m) across, making them unique tools for the study of high energy density physics [1]. Conditions comparable to those in stars, supernova remnants and other astrophysical objects can now be achieved in the laboratory and it is hoped to use such lasers to achieve nuclear fusion [2, 3].

The problem is that the necessarily small volumes and times involved make such experiments very difficult to diagnose, and being able to achieve something is of no interest if you cannot measure it.

Numerous measurements of the heating of plane solid targets by lasers with powers in the TW (10^{12} W) range have been reported [4, 5], but relatively few results are available for

powers approaching a PW [6]–[10], and all of these measurements are either integrated in time or space, or both. Not only that, the exact nature of the temporal and spatial integration of the diagnostics is not clearly defined, being determined by the interval where the temperature was within the detectable range, which inevitably has lower and upper values, and the sensitivity of the particular diagnostic to temperature, which is rarely linear.

Temperatures approaching 60 MK, or 5 keV in terms of kT/e (1 eV = 11 400 K), have been inferred from two separate measurements of line emission from the front (laser side) of solid targets in experiments on the Vulcan petawatt laser [6, 7], using powers of up to 0.5 PW and peak intensities of up to 4×10^{20} W cm^{-2}. These measurements were spatially and temporally integrated, but by the use of layered targets it was found that the temperature fell to much lower values over a distance of less than 1 μm. Such a high temperature over such a thin region could only be maintained for the laser pulse duration of $\sim$1 ps (10^{-12} s).

The most detailed study of the temperatures achieved within plane, solid targets at powers close to a PW is that of Evans *et al* [8]. These results come from an earlier experiment on the Vulcan petawatt laser, which achieved a maximum power of 0.38 PW (300 J in 0.8 ps), focused to a 10 μm full width at half maximum (FWHM) spot to give an intensity of up to 10^{20} W cm^{-2}. They measured the H- and He-like lines emitted from 0.2 μm thick Al layers covered with 4–54 μm of plastic (CH) on the front and 4 μm on the rear. The spectra were spatially integrated and temporally resolved, with a resolution of 14 ps. They found that the emission lasted from 20–50 ps, depending on target thickness. The highest temperature they inferred at solid density was $kT/e = 0.6$–0.75 keV (6.84–8.55 MK) for an 8.2 μm thick front layer. For the 4 μm thick front layer, they obtained $kT/e = 0.6$–0.7 keV at roughly half solid density, which must have been the result of expansion of the target caused by the laser pre-pulse.

Temperatures of the order of 10 MK (keV) at solid density have been obtained over an extended, more accessible region by using thin wires instead of foils [11, 12]. A temperature of $kT/e = 2$–4 keV (22.8–45.6 MK) has been inferred for a 5 μm diameter carbon wire attached to a gold cone with a 30 μm diameter tip [11] irradiated by a laser pulse with a power of 0.23–0.3 PW (180 J in 0.6–0.8 ps). Measurements of the plasma expansion around the wire were compared with hydrodynamic modelling of the expansion of an infinitely long cylinder with initially uniform temperature and density, so it indicates the maximum temperature that was achieved. However, subsequent modelling and experiments have shown that the heating in such targets is concentrated in a thin surface layer [12].

Here, we present the first practically direct measurements of the heating of large area, plane solid targets at powers of 0.32–0.73 PW with *well-defined* spatial *and* temporal resolutions.

2. Experimental methods

The experiments were carried out on the Vulcan petawatt laser [13]. The laser parameters used are given in table 1. P-polarization and an angle of incidence of 40° to the target normal were used. The laser has a pre-pulse with a peak intensity 4×10^{-8} times the peak intensity of the main pulse. A more detailed description of the pre-pulse characteristics is given in [14, 15].

The composition and thickness of the targets used are given in table 1. They were 2 mm wide and 7 mm long strips with the bottom 5 mm attached to a mounting stalk, except for the Mo(1)Ni(0.5)Mo(2.5)V(1) targets, which were 0.4×0.4 mm^2 squares.

Optical emission from the rear surface of the targets was measured using a high speed sampling camera (HISAC) [16], which consists of a fibre optic bundle coupled to an optical

Table 1. Laser energy (E) in joules, laser pulse duration (t, FWHM) in picosecond, peak laser intensity (I_p) in units of 10^{20} W cm^{-2}, target materials and thickness in microns (first material is that irradiated by the laser, CH is polyethylene), target areal electron density ($\int n_e\,dz$) in units of 10^{25} electrons m^{-2} and measured peak rear surface temperature (kT/e) in electronvolt. The star indicates the results that have been extrapolated due to saturation of the signal. The FWHM of the laser spot was approximately 7 μm and the laser wavelength 1.053 μm.

E	t	I_p	Material (thickness)	$\int n_e\,dz$	kT/e
314	0.75	2.93	V(12)Ni(5)	3.27	550 ± 130
224	0.75	2.99	Al(75)Cu(5)Al(1)	7.18	21 ± 6
376	0.75	3.51	Al(50)Cu(5)Al(1)	5.22	270 ± 60
347	0.75	3.24	Al(1)Cu(5)Al(50)	5.22	13^{+10}_{-6}
308	0.75	2.87	CH(4)Al(0.2)CH(4)	0.274	790 ± 50
318	0.75	2.97	Mo(1)Ni(0.5)Mo(2.5)V(1)	1.24	310 ± 70
236	0.75	2.20	CH(8)Al(0.2)CH(4)	0.403	190 ± 60
229	0.75	2.14	CH(12)Al(0.2)CH(4)	0.532	500 ± 130*
365	0.75	3.41	Mo(1)Ni(0.5)Mo(2.5)V(1)	1.24	320 ± 90*
291	0.45	4.53	Al(50)Cu(5)Al(1)	5.22	45 ± 11
225	0.45	3.50	Al(10)Cu(2)Al(1)	1.35	700 ± 170
214	0.45	3.33	Al(30)	2.35	130 ± 50*
188	0.45	2.92	Al(75)	5.87	25 ± 8*

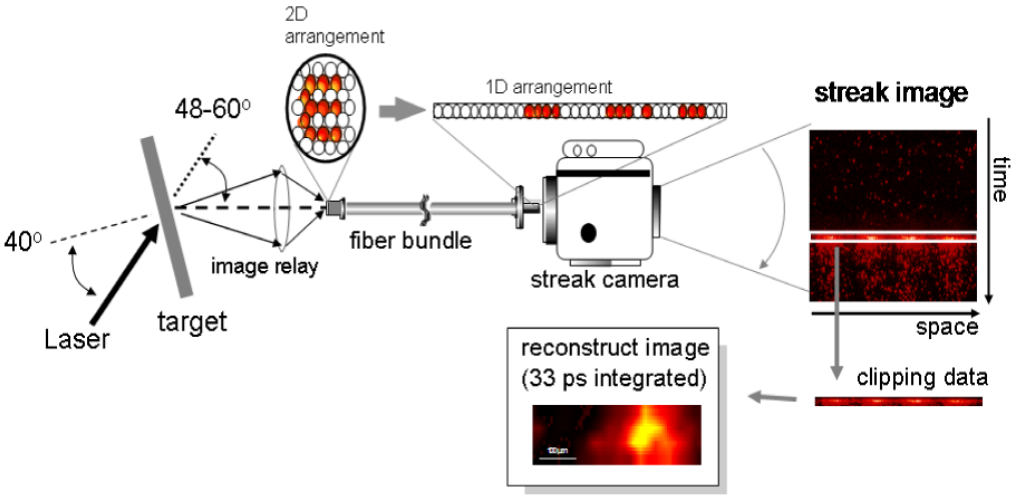

Figure 1. Illustration of the experimental set-up.

streak camera, as illustrated in figure 1. At the entrance slit the fibres are arranged in a one-dimensional array, which can be reconstructed to provide a two-dimensional, time-resolved image. The spatial resolution was limited to 30 μm by the diameter and the number of the fibres. The temporal resolution was limited to 17 ps, half width at half maximum (HWHM), by the dispersion introduced by the diameter and length of the fibres and by the streak camera sweep

speed of 2 ns per 512 pixels. On the shot with the V(12)Ni(5) target a slower sweep speed of 5 ns per 512 pixels was used. The wavelength range of 350–650 nm was limited by the photocathode sensitivity of the streak camera and by the filters used. Optical transition radiation (OTR), which is produced when electrons accelerated into the target by the laser ('fast electrons') cross the rear surface, was excluded from the detector by the use of dichroic filters, with a transmission of 10^{-5} at 527 nm and a notch bandwidth of 75 nm FWHM, since OTR has been found to peak at the second harmonic with a bandwidth of 20–40 nm FWHM [17], and by placing HISAC at 48° or 60° to the laser axis and at 8° or 20° to the target normal, since OTR is emitted in the direction of the fast electrons [18], which tend to be accelerated either along the laser axis or the target normal. In this manner, HISAC measured predominantly thermal optical emission from the rear surface. The intensity of thermal optical emission is, to a good approximation, directly proportional to the temperature (strictly speaking, the radiation temperature) for $kT/e > 10$ eV.

HISAC was not absolutely calibrated, due to the difficulty of obtaining a sufficiently bright, well-characterized source, so the intensities were converted to temperatures by comparison with the fitting of H- and He-like Al lines measured on the shot with the CH(4)Al(0.2)CH(4) target. The fitting was carried out using a time-dependent, collisional-radiative atomic physics model that included opacity, Stark broadening and instrument resolution effects [19], giving the temperature of the Al layer to be 0.79 ± 0.05 keV, at solid density. Thermal conduction was calculated to equilibrate the temperature throughout the target in a few ps, which is well within HISAC's temporal resolution, so this should correspond closely to the peak rear surface temperature. Values for the other targets were calculated by scaling this result according to the ratio of the peak intensities, calculated from the mean of the 63 pixels (9 in the temporal direction, 7 in the spatial direction) that correspond to a single fibre optic, including the standard error. The peak intensity was saturated in some shots, so it was estimated by fitting the non-saturated part of the spatial image with a Gaussian, since this was found to give a good fit to the peaks obtained in the other shots, resulting in larger errors. The emission intensity for the Al(1)Cu(5)Al(50) target, which had the weakest signal, showed several peaks, which were used to obtain upper and lower values. Measurements of V line emission from the Mo(1)Ni(0.5)Mo(2.5)V(1) targets indicated that the rear surface temperature was below 0.4 keV [7], which is consistent with this temperature calibration.

3. Results and discussion

HISAC provides a vast amount of data, here we will concentrate on the peak rear surface temperatures and their dependence on the target thickness and areal density (ρR as it is referred to in inertial fusion), given in table 1. However, before considering these results we will look at some sample spatial images and temporal profiles, given in figure 2, for the thinnest and thickest targets used.

The FWHM of the emission intensity is approximately 160 μm in each case, although it is slightly greater for the Mo(1)Ni(0.5)Mo(2.5)V(1) target, as illustrated by the line-outs given in figure 2. Similar results were obtained for the other shots, with the FWHM falling slightly with increasing target thickness. Both the magnitude of the FWHM and its small decrease with increasing target thickness agrees with results from time integrated imaging of XUV emission (68 eV) from the rear of Cu targets, obtained in another experiment on the Vulcan petawatt laser [15]. The temporal profiles of the peak emission for both targets have a similar rise time, given by the HWHM temporal resolution of 17 ps, so we can only conclude that the heating

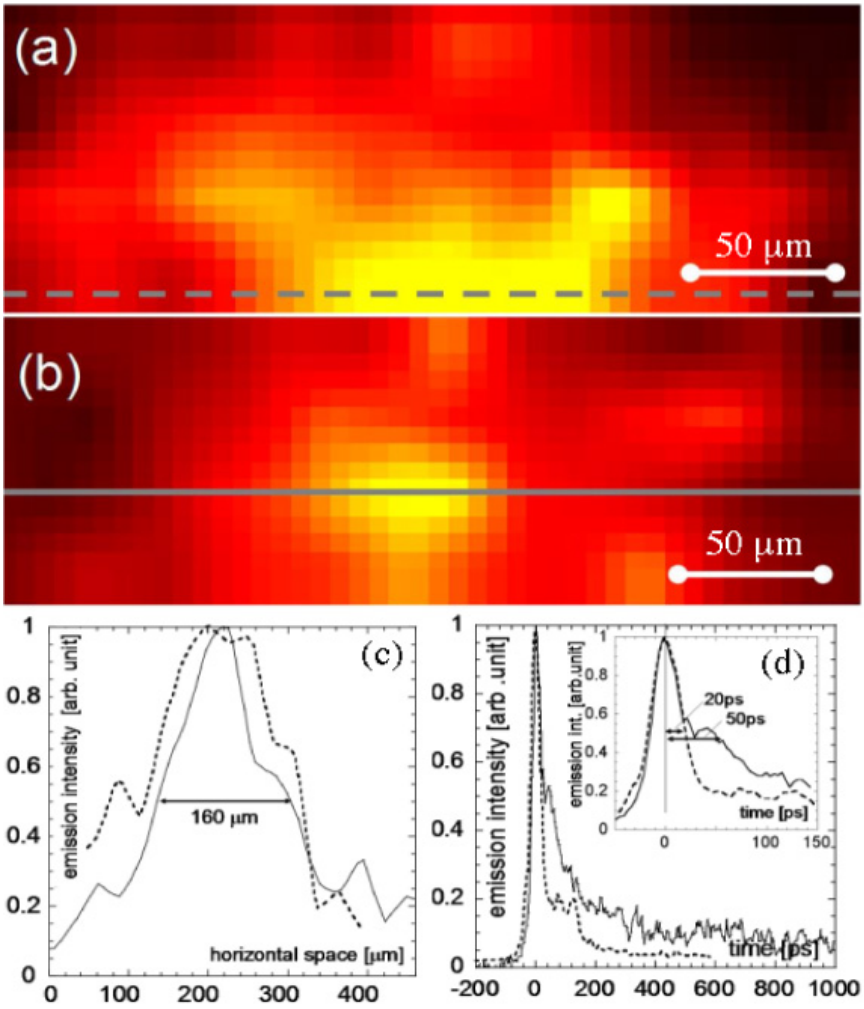

Figure 2. Spatial images from HISAC at the temporal peak of the emission. (a) Mo(1)Ni(0.5)Mo(2.5)V(1) 318 J, (b) Al(75)Cu(5)Al(1) 224 J, (c) intensity along the indicated lines, (d) temporal evolution of the peak emission intensity; dotted line case (a), solid line case (b). The inset shows the evolution between −50 to 100 ps. Zero time is arbitrary.

time is significantly less than 17 ps in all cases. The fall-off times are greater than the temporal resolution and it can be seen that the emission falls to half its maximum value in 20 ps for the Mo(1)Ni(0.5)Mo(2.5)V(1) target and 50 ps for the Al(75)Cu(5)Al(1) target, which represent the smallest and largest values obtained. Again, similar results were obtained in all shots, with the fall-off time increasing with target thickness. This is very close to the duration of the x-ray emission reported by Evans *et al* [8], obtained in a previous experiment on the Vulcan petawatt.

If we use the simple model of an adiabatic expansion with the adiabatic index for three dimensions and ignore lateral expansion, we find that the temperature falls to half its initial value in $89\sqrt{A/Z}L_{\mu\mathrm{m}}/\sqrt{kT/e}$ ps, where A is the ion mass number, Ze is the ion charge, $L_{\mu\mathrm{m}}$ is the target thickness in microns and kT/e is the temperature in electronvolt. Taking $A/Z = 2$,

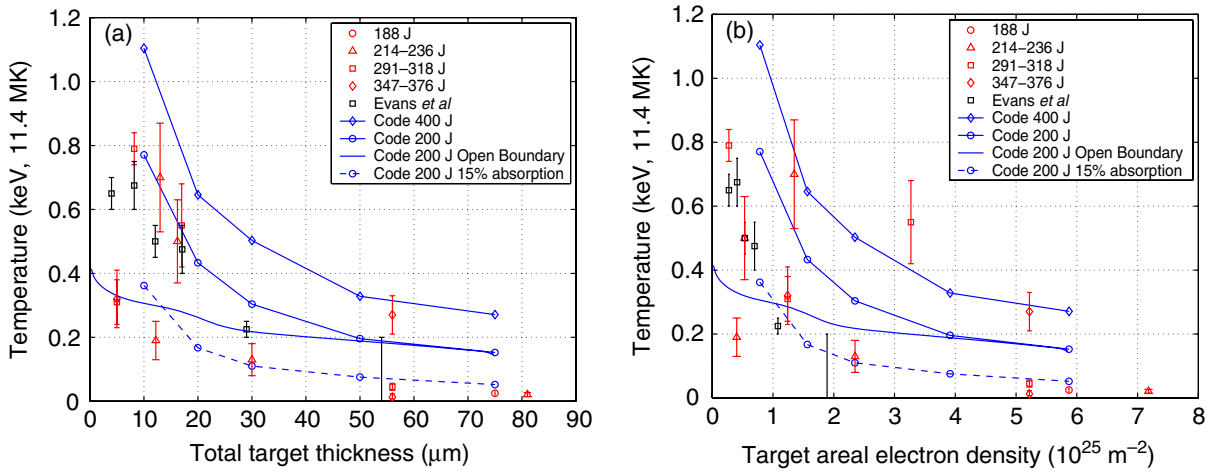

Figure 3. Measured, peak rear surface temperatures as a function of (a) target thickness and (b) areal electron density with the results from Evans *et al* [8] and the results of hybrid code modelling. Note that the scale is linear not logarithmic, so the variations in temperature are more notable.

which will underestimate the expansion time since this is the minimum value that could occur, gives 36 ps for the Mo(1)Ni(0.5)Mo(2.5)V(1) target and 2.2 ns (10^{-9} s) for the Al(75)Cu(5)Al(1) target. Even assuming uniform expansion in all directions still gives a fall-off time of almost a nanosecond for the Al(75)Cu(5)Al(1) target. This clearly indicates that the observed fall-off in temperature is too fast to be explained by bulk target expansion for all but the thinnest targets. The distinct double gradient seen for the Al(75)Cu(5)Al(1) target, with an initial fall-off similar to that for the Mo(1)Ni(0.5)Mo(2.5)V(1) target, is also difficult to explain in these terms. This would appear to be explained by the results of one-dimensional hydrodynamic modelling of XUV emission from the rear of Al targets reported by Gu *et al* [9]. They state that plasma expansion on the rear surface led to an initial fall-off in the emission that depended on initial temperature, not target thickness, and that there was then a subsequent, slower fall-off due to bulk target expansion, which depended on both initial temperature and target thickness. A simple explanation for this result is that initially there is only a pressure gradient at the surface, so this is where the expansion starts. Eventually, this expansion leads to a smooth profile in the pressure gradient throughout the target, and the simple model of bulk expansion will then be applicable. This initial fall-off would appear to be less than HISAC's HWHM temporal resolution of 17 ps, since it is almost identical for the Mo(1)Ni(0.5)Mo(2.5)V(1) and the Al(75)Cu(5)Al(1) targets.

Another factor, which has yet to be considered, is the fast electron driven plasma expansion at the rear of the target. However, since the fast electrons are generated in a pre-plasma formed at the front of the target their initial density cannot exceed the laser critical density, so we would expect the fast electron driven plasma at the rear of the targets to be transparent to optical emission, although it may still refract the emission.

The peak rear surface temperatures are plotted as a function of total target thickness and total areal electron density in figure 3. The reason for using the total areal electron density is that it determines the fast electron stopping power due to collisions and the number of electrons in front of the laser spot that would have to be heated to give the observed temperature, so it gives

a better means of comparing different target materials. It does not account for the changes in the heat capacity with temperature, but there is no simple means of accounting for this. It is clear from figure 3 that it gives a far more consistent trend than target thickness. However, electron stopping by electric field generation is more directly related to the actual distance travelled, so it is also useful to consider the variation of temperature with thickness. For example, considering only Ohmic heating and assuming Spitzer resistivity it can be shown that for strong heating temperature is proportional to $n_e^{-0.4}$, not n_e^{-1} [20]. This means that when comparing targets with the same areal density one with a higher density would be expected to have a higher temperature if Ohmic heating is significant. Indeed, it is notable in figure 3 that the V(12)Ni(5) target appears to have an anomalously high temperature in terms of areal density, but not in terms of thickness, and Ni has the highest electron density of all of the rear surface materials used (in units of 10^{30} m^{-3} the electron density of Ni is 2.56 compared to 0.323 for CH, 0.783 for Al and 1.66 for V).

Despite the fact that the variation in target materials is not entirely accounted for by the areal density, a general trend is clearly visible with the temperature falling sharply with areal density up to about 1.5×10^{25} m^{-2} and relatively slowly thereafter. This trend is also reflected in the temperature variation with target thickness, the transition in the gradient being at around 30 μm.

The points have been grouped according to the laser energy, and this indicates a tendency for the temperature to increase with laser energy. The clearest indication of this is given by the results for the Mo(1)Ni(0.5)Mo(2.5)V(1) and Al(50)Cu(5)Al(1) targets, where a comparison can be made for identical targets with different laser energies.

The results of Evans *et al* [8], obtained in a previous experiment on the Vulcan petawatt, have been included in figure 3. They agree well with our results, showing the same sharp initial fall in temperature with areal density (thickness), but for the thickest target, CH(54)Al(0.2)CH(4), they could only conclude that the temperature was below the detection threshold of 0.2 keV, so the subsequent slower fall cannot be seen. Their result for a CH(4)Al(0.2)CH(4) target falls below this trend and below our result for an identical target, but in this case they found that the density of the Al layer was below solid density, which did not occur in our case. This indicates that there was a lower pre-pulse level in our experiments, allowing the heating of thinner solid targets.

The results for the CH(8)Al(0.2)CH(4) and Al(1)Cu(5)Al(50) targets clearly fall below the general trend. The reason for this is not clear, particularly given the much higher temperatures we obtained with CH(4)Al(0.2)CH(4) and Al(50)Cu(5)Al(1) targets and that Evans *et al* [8] obtained with a CH(8.2)Al(0.2)CH(4) target.

4. Numerical modelling

In order to gain some insight into the fast electron generation and transport from these results they were modelled with the hybrid code as described for previous experiments on Vulcan [15, 21, 22]. This code models the propagation of a specified distribution of fast electrons through a static, uniform solid or plasma (background) including drag, angular scattering and electric and magnetic field generation, calculated using a specified electrical resistivity and heat capacity for the background. The most complete description of the code is given in [23].

The only changes made from the set-up described in [15, 21, 22] were the addition of background thermal conduction and a q-Gaussian [24] instead of a Gaussian for the radial

intensity profile. The reasons for this latter change was that Patel *et al* [10] measured the intensity profile for the Vulcan petawatt and found that 20% of the energy was contained within the FWHM of 6.9 μm and 50% within 16 μm. These figures are reproduced by the q-Gaussian $[1 + (r/4.4539\,\mu\text{m})^2]^{-1.4748}$, whereas a Gaussian would contain 50% of the energy within the FWHM and 97.6% within 16 μm. This was found to be essential to accurately reproduce the spatial profile of the heated region.

Energies on target of 200 and 400 J, a FWHM pulse duration of 0.7 ps, giving peak intensities of 2 and $4 \times 10^{20}\,\text{W cm}^{-2}$, and Al targets of thickness 10, 20, 30, 50 and 75 μm were considered.

Only Al was considered since 7 out of the 13 shots were obtained for targets consisting entirely or primarily of Al, with only 3 being obtained for primarily non-metallic targets, and experimental data for the electrical resistivity of solid Al over the temperature range of interest is available, which is not the case for most other materials. Layered targets were not considered, because the discontinuities they introduce present considerable numerical difficulties and the results obtained are very sensitive to the relative values of the electrical resistivity used, which are not well known [21].

To roughly account for the spatial resolution of the experimental results, we considered the temperature averaged over a radius of 30 μm. It was found that averaging over any radius greater than 10 μm gave a very similar variation of rear surface temperature with target thickness, the curves were simply shifted up as the radius was reduced. The peak temperatures were up to five times higher than these averaged values, but would require micron spatial resolution and picosecond temporal resolution to be observed.

The average rear surface temperatures rose rapidly in 4–5 ps, taking longer for thinner targets, and then very slowly for the next 8–9 ps, when the runs were terminated, since target expansion, which is not included, would then be significant. This means that the code cannot model the observed temporal fall in the rear surface temperatures. The initial rise was due to fast electron heating and its duration was determined by the length of time that the fast electrons spent repeatedly crossing the region being considered as they were reflected between the front and rear surfaces, a process referred to as refluxing. This also led to the heated region being significantly broader than the laser spot and broader for thinner targets, in agreement with the experimental results. The subsequent rise was due to thermal conduction equilibrating the average temperature across the targets. The average temperatures at the front surface following the initial fast electron heating were from 1.2–2.9 times higher than those at the rear surface, increasing with target thickness.

The dominant heating mechanism in all cases was Ohmic heating. The fraction of the fast electron energy deposition that was due to Ohmic heating in the volume defined by the target thickness and the grid radius of 100 μm was from 58.6–62.4% at the low intensity and from 62.0–65.3% at the high intensity, increasing with target thickness. The reduction for thin targets is much lower than might be expected due to current cancellation by fast electrons reflected from the rear surface. This is because the counter-streaming currents led to filamentation in the 10, 20 and 30 μm thick targets, the effect being more pronounced for the thinner targets. The filaments had a size of a few microns so would not be resolved by HISAC. However, the dominant energy loss mechanism in this volume was fast electrons being removed at the radial boundary, which accounted for almost 80% of the total fast electron energy in all cases, varying weakly with intensity and target thickness. In practice this means that the fast electrons would deposit their energy throughout the whole target volume.

The average rear surface temperatures obtained at the end of the runs are included in figure 3. They agree remarkably well with the experimental results, particularly taking into account the simplicity of the model and that no adjustment was made to the fast electron parameters used, those which have given good agreement with previous experiments [15, 21, 22] being used, that is, 30% absorption of laser energy into fast electrons, a 30° cone half angle and a local mean energy given by twice the ponderomotive potential in the strongly relativistic limit.

The most significant point of agreement is the double gradient. This occurred because refluxing considerably increased the target heating for the thinner targets but not for the thicker targets (50 and 75 μm), where the magnetic field generated by the fast electrons entering the target turned the majority of the reflected fast electrons outwards [25]. In the thinner targets the magnetic field did not reach a sufficient value to deflect the fast electrons out of the region considered before they returned from the rear surface. The contribution of refluxing to the double gradient is clearly demonstrated by the result obtained when electrons were removed at the rear surface (open boundary), shown in figure 3, which gives the average temperature within a 75 μm thick target before thermal conduction started to smooth the temperature gradient, since with open boundaries the target thickness has little effect on the target heating. This is an important result because assumptions on refluxing have been found to significantly affect the interpretation of experimental results [4]–[6], especially calculations of absorption. Notably, Akli *et al* [5] found that they had to turn off refluxing at a target thickness of 30 μm, but not at 20 μm or less, in order to reproduce their measurements with a model that did not include magnetic field generation. Our results provide a physical explanation for this.

In practice total refluxing would not occur, because a small fraction of the fast electrons will escape and the rest will lose energy to driving a plasma expansion (ion acceleration), which would also lead to the point of reflection moving outwards in time and being further from the target surface for higher energy electrons. This means that the code would be expected to overestimate the temperature of the thinner targets, which does appear to be the case.

The code results do not agree well with the experimental results in the variation of temperature with laser energy (intensity), which is much smaller in the code results, and for the thicker targets, where the code results are much higher. By coincidence, the results for the thicker targets were obtained with the lowest laser energies. The discrepancy for the thicker targets is particularly worrying because these are Al targets and the code results are unaffected by assumptions on refluxing, so the code would be expected to accurately reproduce these results. We investigated if this could be explained by some additional variation in the fast electron parameters with laser energy (intensity) by varying the absorption [26], cone angle [27] and mean energy [28], individually, by a factor of 2 either way, since such variations have been reported. Only the variation in absorption produced a sufficient variation in the rear surface temperatures, the other parameters had remarkably little effect. This means that the most important parameter in determining the average rear surface temperature is the total fast electron energy entering the target.

The results for 200 J laser energy and 15% absorption (30 J fast electron energy) are included in figure 3. Combined with the results for 400 J and 30% absorption (120 J fast electron energy) they clearly give much better agreement with the experimental results as a whole. The agreement of the results for the thicker targets has improved dramatically, due to a factor of 3 reduction in the code results. One of the reasons for this is that at these low temperatures the resistivity of Al increases with temperature, which leads to a very strong dependence of Ohmic heating on current density [20].

An absorption of 60% clearly disagreed with the experimental results; not only did it give higher temperatures it also gave a slower, linear decrease in temperature with target thickness without the distinctive double gradient.

Given the sensitivity of the temperature variation with target thickness to absorption and its relative insensitivity to cone angle and mean energy within widely accepted values we can conclude, with some confidence, that the absorption lies in the range 15–30% and that it tends to increase with laser energy, for our parameters. We can also conclude that a relatively small shot-to-shot variation in absorption would be sufficient to explain the fluctuations observed in the experimental results, whereas a very large variation in cone angle or mean energy would be required. This variation in absorption could well occur due to shot-to-shot variations in the pre-pulse [15].

The absorption of laser energy has been inferred in numerous experiments with laser powers greater than a TW, and the values obtained range from 10–80% [3]–[11], [26]. This wide variation is not what it first seems, because some results refer to total absorption while others, such as ours, refer only to the absorption into electrons entering the solid. The values inferred for this latter fraction, which is the value of interest for target heating, fast ignition, rear surface ion acceleration and many other applications, tend to fall in the range 10–30%, in agreement with our results. However, taken as a whole, these results show no clear trend, whereas measurements of total absorption [26] clearly indicate an increase with laser intensity, a tendency that is partially supported by our results. These measurements of total absorption indicate values of 60–80% for our case. This indicates that most of the absorbed laser energy does not go into electrons entering the target. The main additional energy sink at the front of the target is most likely ion acceleration, both into and out of the target (the latter could also be referred to as plasma formation), so this would appear to be increasing significantly with laser intensity. Another possible explanation is some form of inhibition of fast electron propagation. It has been found in modelling with other hybrid codes that a few microns of plasma between the critical surface and the solid is sufficient to significantly reduce the fast electron energy entering the solid [8, 29]. The excitation of ion instabilities is another possible explanation [30]. However, more precise information on laser absorption into all possible channels is required before any definite conclusions can be drawn.

5. Conclusions

In conclusion, we have measured the thermal optical emission from the rear surface of solid targets following irradiation by laser pulses with powers from 0.32–0.73 PW and intensities of up to 4×10^{20} W cm^{-2} with spatial and temporal resolutions of 30 μm and 17 ps, respectively. These measurements show that a region 160 μm in diameter and up to 20 μm thick can be heated to a temperature of the order of 10 MK ($kT/e \sim$ keV) at solid density and that this temperature is maintained for at least 20 ps. More importantly, we have shown that it is possible to diagnose the necessarily small temporal *and* spatial scales required to produce such high energy densities in the laboratory.

Hybrid code modelling has shown that magnetic field generation prevents increased target heating by electron refluxing above a certain target thickness and that the absorption of laser energy into electrons entering the solid target was between 15–30%, and tends to increase with laser energy.

Acknowledgments

This work was supported by the UK EPSRC and STFC. MN and RK were supported by the CREST, Japan Science and Technology Agency. JRD was supported by the FCT, grant POCI/FIS/59563/2004. American colleagues acknowledge support from the US Department of Energy, contracts W-7405-Eng-48 and DE-FC52-08NA28302. The authors gratefully acknowledge the support of the staff of the Central Laser Facility, Rutherford Appleton Laboratory.

References

[1] Board of Physics and Astronomy 2003 *Frontiers in High Energy Density Physics: The X-Games of Contemporary Science* (Washington, DC: National Academies Press)
[2] Tabak M *et al* 1994 *Phys. Plasmas* **1** 1626
[3] Campbell E M, Freeman R R and Tanaka K A 2006 *Fusion Sci. Technol.* **49** 249
[4] Chien C Y, Coe J S, Mourou G, Kieffer J C, Chaker M, Beaudoin Y, Peyrusse O and Gilles D 1993 *Opt. Lett.* **18** 1535
Jiang Z *et al* 1995 *Phys. Plasmas* **2** 1702
Saemann A, Eidmann K, Golovkin I E, Mancini R C, Andersson E, Förster E and Witte K 1999 *Phys. Rev. Lett.* **82** 4843
Koch J A, Key M H, Freeman R R, Hatchett S P, Lee R W, Pennington D, Stephens R B and Tabak M 2001 *Phys. Rev.* E **65** 016410
Martinolli E *et al* 2002 *Laser Part. Beams* **20** 171
Andiel U, Eidmann K, Hakel P, Mancini R C, Junkel-Vives G C, Abdallah J and Witte K 2002 *Europhys. Lett.* **60** 861
Eidmann K, Andiel U, Pisani F, Hakel P, Mancini R C, Junkel-Vivesc G C, Abdallah J and Witte K 2003 *J. Quantum Spectrosc. Radiat. Transfer* **81** 133
Nishimura H *et al* 2003 *J. Quantum Spectrosc. Radiat. Transfer* **81** 327
Martinolli E *et al* 2006 *Phys. Rev.* E **73** 046402
Chen S N *et al* 2007 *Phys. Plasmas* **14** 102701
[5] Akli K U *et al* 2007 *Phys. Plasmas* **14** 023102
[6] Theobald W *et al* 2006 *Phys. Plasmas* **13** 043102
Myatt J *et al* 2007 *Phys. Plasmas* **14** 056301
[7] Key M H *et al* 2006 *J. Physique* IV **133** 371
[8] Evans R G *et al* 2005 *Appl. Phys. Lett.* **86** 191505
Evans R G *et al* 2004 *Central Laser Facility Annual Report 2003–2004* (CCLRC ISSN 1358-6254) p 12
[9] Gu P *et al* 2006 *Rev. Sci. Instrum.* **77** 113101
[10] Patel P K *et al* 2005 *Plasma Phys. Control. Fusion* **47** B833
[11] Kodama R *et al* 2004 *Nature* **432** 1005
[12] Green J S *et al* 2007 *Nat. Phys.* **3** 853
Pasley J *et al* 2007 *Phys. Plasmas* **14** 120701
[13] Danson C N *et al* 2004 *Nucl. Fusion* **44** S239
[14] Musgrave I *et al* 2007 *Appl. Opt.* **46** 6978
[15] Lancaster K *et al* 2007 *Phys. Rev. Lett.* **98** 125002
[16] Kodama R, Okada K and Kato Y 1999 *Rev. Sci. Instrum.* **70** 625

[17] Baton S D *et al* 2003 *Phys. Rev. Lett.* **91** 105001
Jung R *et al* 2004 *Central Laser Facility Annual Report 2003–2004* (CCLRC ISSN 1358-6254) p 31
Popescu H *et al* 2005 *Phys. Plasmas* **12** 063106
Batani D, Manclossi M, Santos J J, Tikhonchuk V T, Faure J, Guemnie-Tafo A and Malka V 2006 *Plasma Phys. Control. Fusion* **48** B211
Santos J J *et al* 2007 *Phys. Plasmas* **14** 103107
[18] Zheng J *et al* 2003 *Phys. Plasmas* **10** 2994
[19] Lancaster K *et al* 2006 *Central Laser Facility Annual Report 2005-2006* (CCLRC ISSN 1358-6254) p 38
[20] Davies J R 2003 *Phys. Rev.* E **68** 056404
[21] Wei M S *et al* 2006 *Phys. Plasmas* **13** 123101
[22] Davies J R, Green J S and Norreys P A 2006 *Plasma Phys. Control. Fusion* **48** 1181
[23] Davies J R 2002 *Phys. Rev.* E **65** 026407
[24] Tsallis C J, Mendes R S and Plastino A R 1998 *Physica* A **261** 534
[25] Davies J R, Bell A R and Tatarakis M 1999 *Phys. Rev.* E **59** 6032
[26] Green J S *et al* 2008 *Phys. Rev. Lett.* **100** 015003
[27] Sentoku Y 2007 *Bull. Am. Phys. Soc.* **52** 269
[28] Key M H *et al* 1998 *Phys. Plasmas* **5** 1966
Wharton K B *et al* 1998 *Phys. Rev. Lett.* **81** 822
Hatchett S P *et al* 2000 *Phys. Plasmas* **7** 2076
Kodama R *et al* 2001 *Phys. Plasmas* **8** 2268
Town R P J *et al* 2005 *Nucl. Instrrum. Methods Phys. Res.* A **544** 61
Ping Y *et al* 2008 *Phys. Rev. Lett.* **100** 085004
[29] Honrubia J J, Kaluza M, Schreiber J, Tsakiris G D and Meyer-ter-Vehn J 2005 *Phys. Plasmas* **12** 052708
[30] Mendonça J T, Norreys P A, Bingham R and Davies J R 2005 *Phys. Rev. Lett.* **94** 245002
Norreys P A *et al* 2005 *Plasma Phys. Control. Fusion* **47** L49
Mendonça J T, Norreys P, Bingham R and Davies J R 2005 *Plasma Phys. Control. Fusion* **47** B799